Moringa Gum-derived Polymeric Carbon Dots for Antimicrobial Activity

Yasir Iqbal [a,b,*] Shahzad Ali Shahid Chatha,[b] Iqbal Ahmed,[b, c] Khuram Shahzad,[a] Muhammad Yasir Siddique,[d] and Usama Anwar [e]

* *Corresponding author: yasirgcu7@gmail.com*

DOI: 10.15376/biores.20.2.4479-4494

GRAPHICAL ABSTRACT

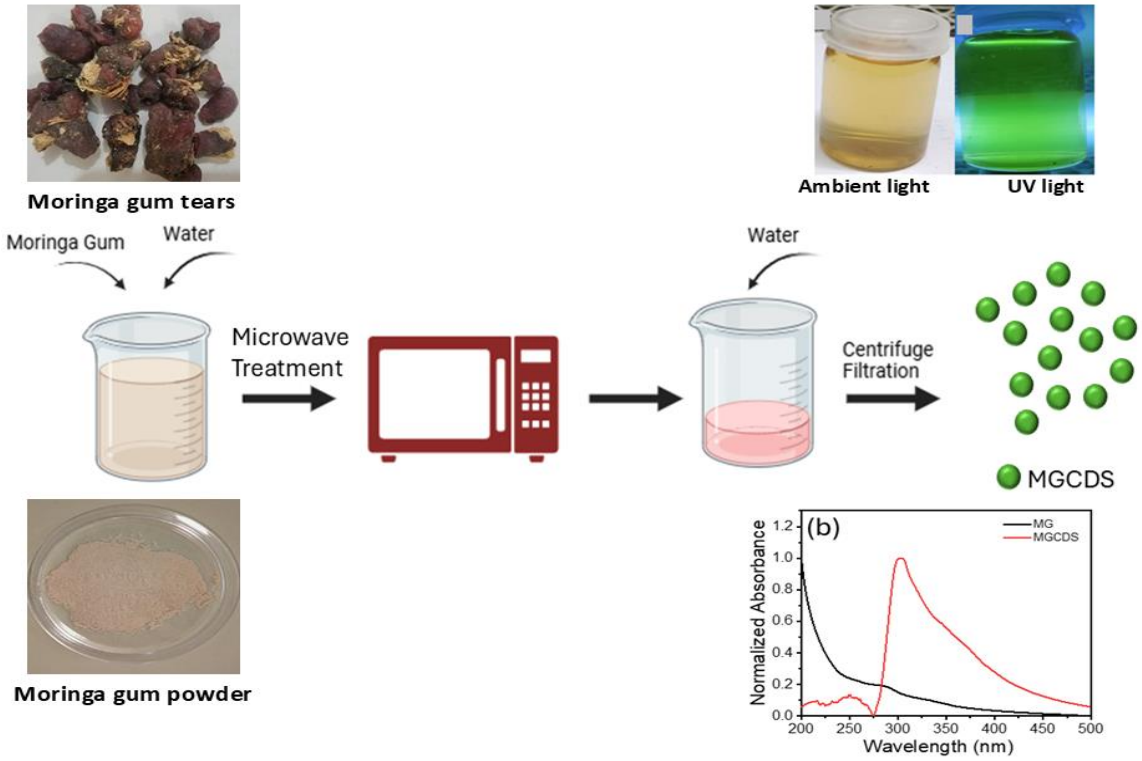

Moringa Gum-derived Polymeric Carbon Dots for Antimicrobial Activity

Yasir Iqbal [a,b]* Shahzad Ali Shahid Chatha,[b] Iqbal Ahmed,[b,c] Khuram Shahzad,[a] Muhammad Yasir Siddique,[d] and Usama Anwar [e]

The scientific community is actively developing innovative nanomaterials with broad-spectrum antimicrobial properties. In this study, moringa gum-derived polymeric carbon dots (MGCDs) were synthesized *via* a rapid and eco-friendly microwave irradiation technique using aqueous moringa gum as the precursor. The resulting MGCDs exhibited strong green fluorescence under UV light, with a UV-Vis absorption peak at ~290 nm and excitation-dependent fluorescence at 360 nm. They demonstrated significant antioxidant activity, achieving 87% DPPH scavenging efficiency at 0.9 mg/mL, comparable to ascorbic acid. Zeta potential analysis confirmed high colloidal stability, with values of 29 ± 0.9 mV (DI water), 30 ± 0.8 mV (SBB), 28 ± 9 mV (PBS), and 23 ± 0.8 mV (DMEM). Hydrodynamic sizes ranged from 86 ± 3 nm to 135 ± 4 nm, indicating solvent-dependent dispersion. TGA showed high thermal stability, while XRD confirmed an amorphous carbon structure with a broad peak at 22°. MGCDs demonstrated the antibacterial activity against *Staphylococcus aureus* and *Bacillus subtilis*, resulting in inhibition zones of 17.4 ± 0.8 mm and 15.2 ± 0.6 mm, respectively, at 40 mg/mL. Their multifunctionality, simple synthesis, and cost-effectiveness highlight their potential in bioimaging, antimicrobial applications, and fluorescent materials.

DOI: 10.15376/biores.20.2.4479-4494

Keywords: Carbon dots; Antibacterial activity; Moringa gum; Microwave synthesis

Contact information: a: Department of Chemistry, Baba Guru Nanak University, Nankana Sahib-39100, Pakistan; b: Department of Chemistry, Government College University Faisalabad-38000, Pakistan; c: Department of Industrial Engineering, University of Rome Tor Vergata, Rome 00133, Italy; d: Department of Chemistry, University of Gujrat, 5700-Gujrat, Pakistan; e: Department of Biomedical Science, University of Sassari, CR-INSTM, Sassari-07100, Italy;
** Corresponding author: yasirgcu7@gmail.com*

INTRODUCTION

Carbon dots (CDs) have attracted a lot of interest due to their unique properties, including excellent stability, biocompatibility, and tunable photoluminescence. These qualities make them ideal for a wide range of applications, such as bioimaging, sensors, drug delivery, and photocatalysis (Emam 2022). These zero-dimensional carbonaceous nanomaterials exhibit unique optical characteristics, such as strong fluorescence, high quantum yield, and excellent photostability, which have led to their widespread use in biomedical and environmental applications (Yang *et al.* 2025). CDs can be classified into carbon quantum dots (CQDs), graphene or graphene oxide quantum dots (GQDs or GOQDs), and carbonized polymer dots (CPDs) (Zhu *et al.* 2015; Daoudi *et al.* 2024). Recent advancements in the synthesis, functionalization, and application of CDs have paved the way for innovative solutions in diverse fields, including nanomedicine,

environmental remediation, and optoelectronics. However, despite significant progress, challenges such as low quantum efficiency, batch-to-batch variability, and limited control over surface functionalization still need to be addressed for broader commercial and clinical applications (Emam and Ahmed 2021; Ahmed *et al.* 2024).

The synthesis of carbon dots (CDs) generally follows two main approaches: top-down and bottom-up methods. In top-down techniques – such as laser ablation, electrochemical oxidation, and arc discharge – larger carbon structures are broken down into nanoscale CDs. On the other hand, bottom-up methods, including hydrothermal, solvothermal, and microwave-assisted techniques, involve assembling CDs from smaller molecular precursors, that facilitate the self-assembly of CDs from molecular precursors (Modi *et al.* 2023). When compared to the conditions of the traditional hydrothermal approach, the microwave (MW) assisted hydrothermal synthesis is a simple strategy for producing luminous CDs with low energy consumption. The inability to effectively manage some variables, such as CD size, limits the effectiveness of this technology. Additionally, the process by which CDs are developed under (MW) irradiation is complicated and not backed by concrete insight (Wang *et al.* 2014; Shibata *et al.* 2022). Functionalization of CDs plays a crucial role in tailoring their properties for targeted applications. Surface modification using heteroatom doping (*e.g.*, N, S, P) has been widely investigated to improve quantum yield, charge transfer efficiency, and stability. Moreover, surface passivation with polymers and biomolecules has enabled enhanced biocompatibility, making CDs highly suitable for biomedical applications such as drug delivery, biosensing, and cancer therapy. The versatility of CDs has also been demonstrated in their use as nanocarriers for anticancer drugs, where their fluorescence properties allow simultaneous imaging and therapeutic functionalities. Studies have reported the successful conjugation of CDs with chemotherapy drugs, leading to improved drug solubility and targeted delivery with minimal cytotoxicity (Ahmed and Emam 2020; Ahmed *et al.* 2023)

Beyond biomedical applications, CDs have shown promise in environmental and energy-related technologies. Their photocatalytic activity has been extensively studied for applications in wastewater treatment, hydrogen production, and CO_2 reduction. The ability of CDs to act as electron donors or acceptors in photocatalytic reactions has led to their integration with semiconductor materials for enhanced charge separation and catalytic efficiency. Additionally, CDs have been employed in the fabrication of light-emitting diodes (LEDs) and solar cells, where their tunable emission properties contribute to improved device performance. Recent works highlight the importance of CDs in enhancing the efficiency of photovoltaic devices by acting as light-harvesting materials with broad absorption spectra (Emam *et al.* 2021; Daoudi *et al.* 2024)

Despite these promising advancements, several challenges remain in the large-scale production, reproducibility, and stability of CDs. The need for standardized synthesis protocols, comprehensive toxicity evaluations, and scalable functionalization strategies is crucial for the successful translation of CDs into real-world applications. Future research should focus on the development of highly efficient and environmentally friendly synthetic routes, deeper mechanistic understanding of CD interactions at the molecular level, and further exploration of their multifunctional capabilities in diverse applications (Ahmed *et al.* 2021; Emam 2024). Polysaccharides, due to their specific carbon core structure and surface groups, serve as an excellent carbon source for carbon dot synthesis, owing to their accessibility, cost-effectiveness, abundance of functional groups, and exceptional biocompatibility. Polysaccharides represent a prominent, diverse, and important category of biological molecules. The abundance, accessibility, and variety of polysaccharides,

together with their significant hydrophilicity, low carbonization temperature, cost-effectiveness, and benign nature, render them favoured precursors for CDs synthesis.With all of the above possibilities for modifying the synthetic technique of CDs, it is not unexpected that researchers have already begun to examine and approve the positive properties of polysaccharides by focusing on the synthesis of new fluorescence-active CDs with improved characteristics (Emam 2022; Bazazi *et al.* 2023). Recent advances in carbon dot (CD) synthesis have focused on sustainable and cost-effective precursors, particularly those derived from undesirable waste materials. Agricultural residues, food waste, and industrial by-products have been widely explored as low-cost alternatives for CD synthesis due to their high carbon content and abundance. Examples include fruit peels, lignocellulosic biomass, and spent coffee grounds, which offer an eco-friendly approach to nanomaterial development (Alabadi *et al.* 2015; Basta *et al.* 2021). Compared to these waste-derived precursors, researchers have been continuously exploring new materials for their possible utilization in biomedical field (Wang *et al.* 2024; Zhou *et al.* 2025), thus in this scenario moringa gum has been utilized that is a mainly composed of polysaccharide with unique functional properties, making it a valuable starting material. While moringa gum-derived carbon dots (MGCDs) exhibit biocompatibility and stability, the use of waste-based carbon sources could further reduce production costs and promote circular economy practices. The moringa gum's natural abundance, eco-friendliness, and rich carbon content (Iqbal *et al.* 2023; Kumar and Singh 2024) make it an ideal base material for the synthesis of moringa gum-based carbon dots. Therefore, in the current study the CDs have been prepared from microwave assisted hydrothermal synthesis with moringa gum as base carbon material. Thus, future studies should explore a comparative analysis of MGCDs with waste-derived CDs to assess their structural, optical, and functional differences, thereby optimizing both sustainability and performance for biomedical and environmental applications. Several studies have explored the synthesis of CDs from natural sources such as carbohydrates, proteins, and plant extracts, demonstrating their potential as cost-effective and biocompatible materials (Emam *et al.* 2023; Bazazi *et al.* 2023; Emam 2024).

EXPERIMENTAL

Materials

This study used ascorbic acid (Ac) (CAS No. 50-81-7) and (DPPH, CAS No. 1898-66-4, molecular weight: 394.32 g/mol). Moringa gum was obtained from Bara Dawakhana, a recognized natural medicine store (PHC Registration No. R-54521 in Faisalabad. The solution was prepared using deionized water. Ciprofloxacin disks (5 µg, CT052B) were bought from Thermo Fisher and utilized as control.

Moringa Gum Derived Carbon Dots Synthesis

A microwave-assisted synthesis (MAS) process was used to create the moringa-based carbon dots (MGCDS). For this 0.2 g of natural polymer was dispersed in deionized water (DI) under constant mixing for two hours to completely dissolve the polymer matrix. The above contents were transferred to the conventional microwave-based oven and heated until the volume of solution remained 1/4th of the original volume. The appearance of the solution changed to reddish dark brown. The solution was exposed to microwave radiation in the oven by means of a heating and cooling cycle, *i.e.*, 30 seconds exposure to the microwave was followed by 5 min of cooling cycle to avoid the overheating of solution.

The 30 to 35 exposures were given, and it took 50 to 60 min for completion of said process. The last step was to bring the mixture to room temperature before adding 10 mL of (DI) and it was stirred for 30 min. The mixture was centrifuged to 5000 revolutions/min for 10 min to remove the larger particles. The resultant supernatant was filtered by 0.2 µ-syringe filter and stored for further use.

Characterizations

Fourier transform infrared spectrometry (FTIR)

The ATR FTIR spectrometer, ThermoScientific Nicolet iS5 (Waltham, MA) was used to analyze the functional groups and chemical interactions within the samples. The analysis covered a spectral range of 4000 to 500 cm^{-1} with a resolution of 2 cm^{-1}, providing an understanding of material interactions. The powdered moringa gum which was used as precursor and synthesized MGCDS were subjected to FTIR analysis.

Ultraviolet – visible spectroscopy (UV-VIS) /Fluorescence spectroscopy (PL)

The (UV-VIS) absorption spectra of samples that needed to be performed were obtained with Lambda 25, Perkin Elmer in range of 200 to 800 nm. The fluorescence spectroscopy was done by Spectro-Fluorophotometer (RF-6000). The excitation wavelengths were 320, 325, and 360 nm. The LabSolutions RF software was used to obtain data.

Thermal analysis

Thermogravimetric analysis (TGA) using the Simultaneous DSC-TGA, SDT Q600 system (New Castle, DE) was used to access the materials' thermal properties and stability. Under a controlled heating rate of 10 °C/min with a constant nitrogen flow of 50 mL/h, the samples were heated from 25 to 600 °C.

X-ray diffraction analysis (XRD)

The degree of crystallinity or amorphous characteristics of the samples was assessed through X-ray diffraction (XRD). XRD spectra were acquired utilizing an X-ray Diffractometer (D8 Bruker system). The samples were positioned in the specified sample holder, and the diffractogram was acquired within the 2θ range of 10° to 80°. Subsequently, the Rietveld refinement of the XRD pattern was performed utilizing a two-phase model in the Fullprof program and plotted using Origin 2022 (Academic).

Zeta potential and hydrodynamic particle size

The zeta potential and particle size analysis of MGCDS was performed by zeta sizer instrument Malvern zeta seizer 2000, at room temperature.

Statistical analysis

To ensure the reliability and reproducibility of the experimental data, descriptive statistical analysis was performed. Mean and standard deviation were calculated for each dataset to assess data dispersion and central tendency. The coefficient of variation (CV) was also determined to evaluate data consistency. All statistical analyses were conducted using OriginPro, and graphical representations such as error bars in plots were included to highlight variability. Each experiment was performed in triplicates (n = 3) to ensure statistical significance.

Biological Activities

DPPH assay

The evaluation of antioxidant activity was conducted utilizing the DPPH scavenging assay. MGCDS and ascorbic acid (Ac) (standard) at different concentrations (0.05 to 0.9 mg/mL) were combined with 1 mL of 0.2 mM DPPH in methanol. The mixture underwent incubation in a dark environment at room temperature for a duration of 30 minutes, followed by the measurement of absorbance at 517 nm. A methanolic DPPH solution was utilized as the blank (Jeong *et al*. 2019). The antioxidant activity was quantified using the following formula,

$$\%\ DPPH\ radical\ inhibition = \frac{Ab.\ of\ blank - Ab.\ of\ sample}{Ab.\ of\ blank} \times 100 \quad (1)$$

where *Ab* is absorbance.

Antibacterial activity

The antibacterial activity of the MGCDS was evaluated against two bacterial strains, *B. subtilis* (ATCC23857) and *S. aureus* (ATCC25923), utilizing the agar well diffusion technique. The bacterial isolates were initially cultivated for 24 hours on tryptic soy agar (TSA) to generate a standardized inoculum. Subsequently, the inoculum was incubated at 37 °C until the concentration of colony forming units (CFU/mL) achieved 1 × 10^9. To inoculate the agar plates, the standardized microbial suspension was evenly spread over the entire surface of plate. A sterile cork borer with a diameter of 6 mm was utilized to create wells in the agar. Subsequently, 100 µL of a 40 mg/mL sample was added to the wells, with ciprofloxacin disk used as a positive control. After a 24-h incubation period, the zones of inhibition (measured in mm) for each sample were recorded. Each zone was measured from three different positions and results were expressed as mean ± standard deviation.

RESULTS AND DISCUSSION

Fluorescent carbon dots were synthesized in an aqueous solution using moringa gum as the precursor and water as the solvent, employing a microwave-assisted technique, as shown in Fig. 1. The synthesis process involved precise control of temperature and microwave radiation cycles, as outlined in the Methods section. The obtained carbon dots were then subjected to structural characterization using a variety of complementary techniques.

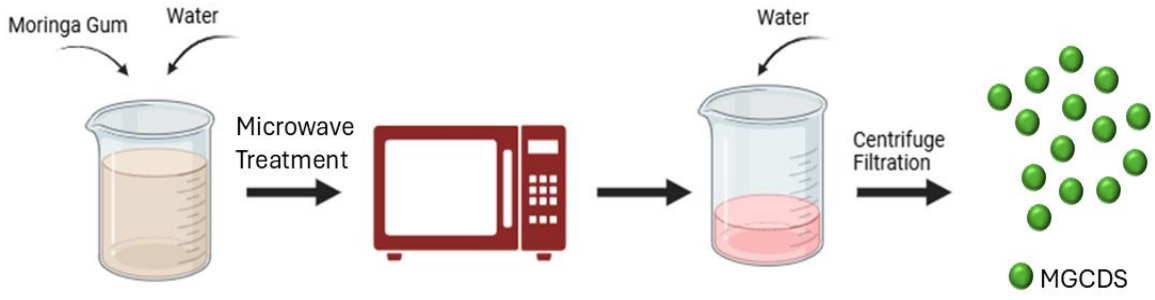

Fig. 1. Carbon dots synthesized by microwave assisted technique

XRD analysis

The XRD examination of MGCDS exhibited a broad peak in region of (2θ = 20 to 30°), which was attributed to the amorphous carbon structures (Fig. 2) (Mohanty *et al.* 2007). The weak diffraction peak in region of (2θ = 40 to 50°) was ascribed to the α axis of graphite structure (Sharma *et al.* 2022). The X-ray diffraction (XRD) pattern of carbon dots was analyzed and refined using the Rietveld refinement method to elucidate their structural properties. The experimental data represented by black markers exhibit distinct diffraction peaks, indicating the presence of crystalline domains within the carbon dots, which was likely originating from graphitic structures. The calculated pattern, shown as a red curve, was obtained by fitting the experimental data using a crystallographic model, providing insights into the structural arrangement. The green ticks represent the Bragg positions, corresponding to the theoretical diffraction angles of the modeled crystal structure, while the blue line indicates the difference between the experimental and calculated patterns. The close alignment of the experimental and calculated data, as evidenced by the minimal deviation in the difference plot, signifies the reliability of the refinement.

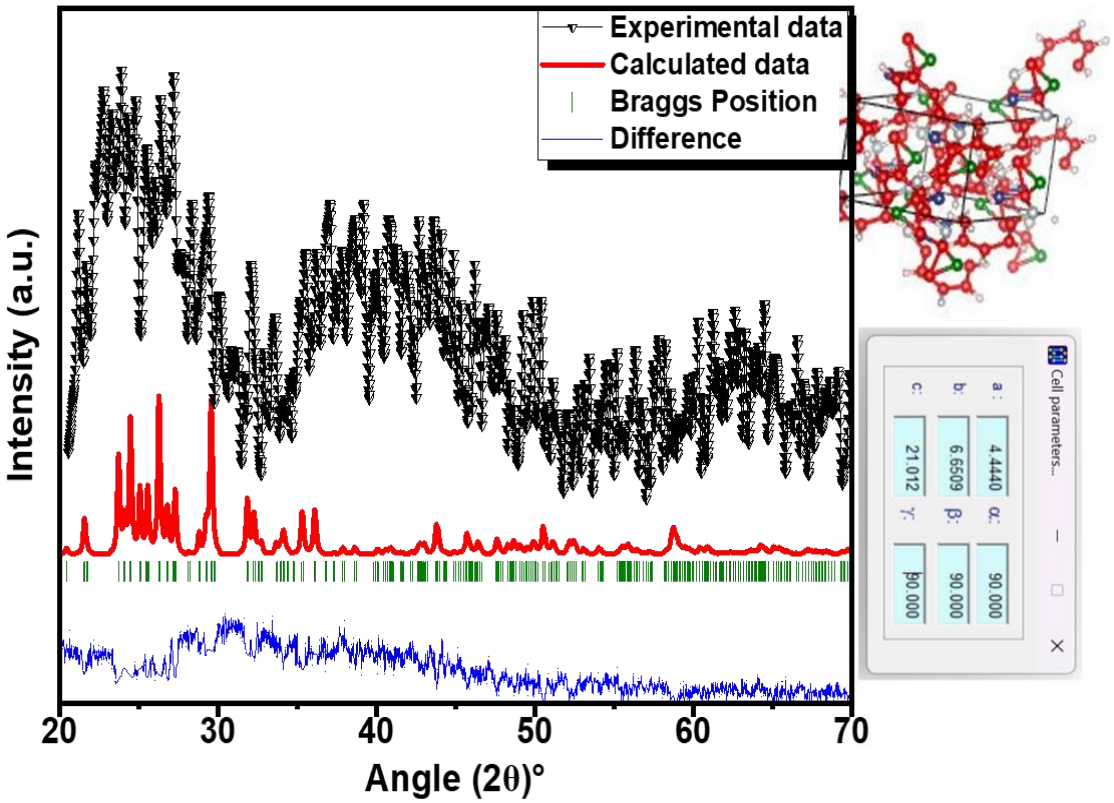

Fig. 2. Rietveld refinement of the XRD pattern for carbon dots. Experimental data (black markers) align well with the calculated pattern (red line), with Bragg positions (green ticks) and a minimal difference plot (blue line)

The data were well matched with its standard diffraction pattern JCPDS (No. 26-1076) and found to be at good agreement. The refinement yielded lattice parameters a=4.4440 A˚, b=6.6590 A˚, and c=21.012 A˚, suggesting a well-defined crystalline structure. The broadening of the peaks indicates the presence of nanocrystalline domains,

consistent with the typical characteristics of carbon dots, which often exhibit a graphitic core surrounded by an amorphous matrix. The size average crystallite size was calculated to be 12 nm by use of Deby Scherrer's formula. The refinement also provides quantitative information about the atomic arrangement, which is crucial for understanding the material's properties. The crystalline features of the carbon dots are significant for their functional applications, such as photoluminescence, catalysis, and bioimaging, where the interplay between crystalline and amorphous phases plays a pivotal role.

Spectroscopic analysis

The FTIR spectra of the synthesized MGCDs exhibit distinct features compared to the base material, MG, as shown in Fig. 3a. A broad peak centered at 3226 cm^{-1}, accompanied by a shoulder at 2929.7 cm^{-1}, is observed. The broad peak in the region of 3400 to 3000 cm^{-1} was attributed to O–H and N–H stretching vibrations, indicative of hydroxyl and amino groups on the carbon dot surface (Ding *et al.* 2017; Kolanowska *et al.* 2022). The shoulder peak at 2929.7 cm^{-1} corresponds to C–H stretching vibrations, while a sharp peak at 1559.9 cm^{-1} can be assigned to N–H deformation vibrations (Nair *et al.* 2020; Kaczmarek *et al.* 2021). Additionally, the peak at 1405 cm^{-1} is associated with C=C stretching and the sharp peak at 1017.6 cm^{-1} represents the symmetric vibration of the C–O–C bond (Zhang *et al.* 2012; Wang *et al.* 2014).

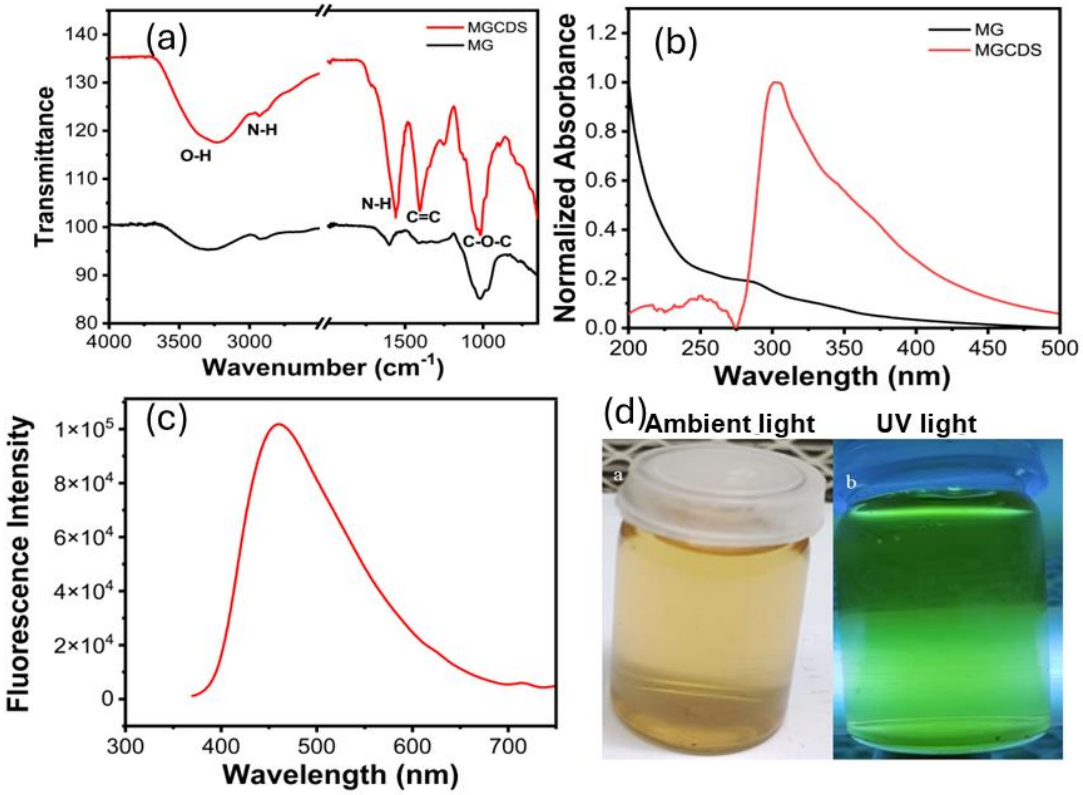

Fig. 3. (a) FITR spectra of MG and MGCDS. (b) UV-visible spectra of MG and MGCDS. (c) PL spectra of MGCDS (λ_{ex}: 360 nm). (d) Photographs of MGCDS solution under ambient and UV light

Figure 3b shows the UV-VIS spectra of MGCDS. The absorbance peak was centered at 300 nm with the tail extending towards the visible region. The features observed in this spectral range are commonly attributed to either π–π* or n–π* transitions associated

with carbonyl groups or related functional groups. Such transitions typically result in emission bands appearing in the visible region of the spectrum (Demchenko 2019; Sharma *et al.* 2017). The fluorescence emission of carbon dots exhibits a strong overlap with their absorbance spectrum, with a maximum emission at 460 nm under the 360 nm excitation which has been elaborated in Fig. 3c. Further emission spectra with relative to excitation at different wavelengths have been elaborated in Fig. 4. The emission profile is broad, extending into the green region. This emission behavior is further illustrated in Fig. 3d, where a photograph of the MGCDS dispersion in water shows green fluorescence under UV light.

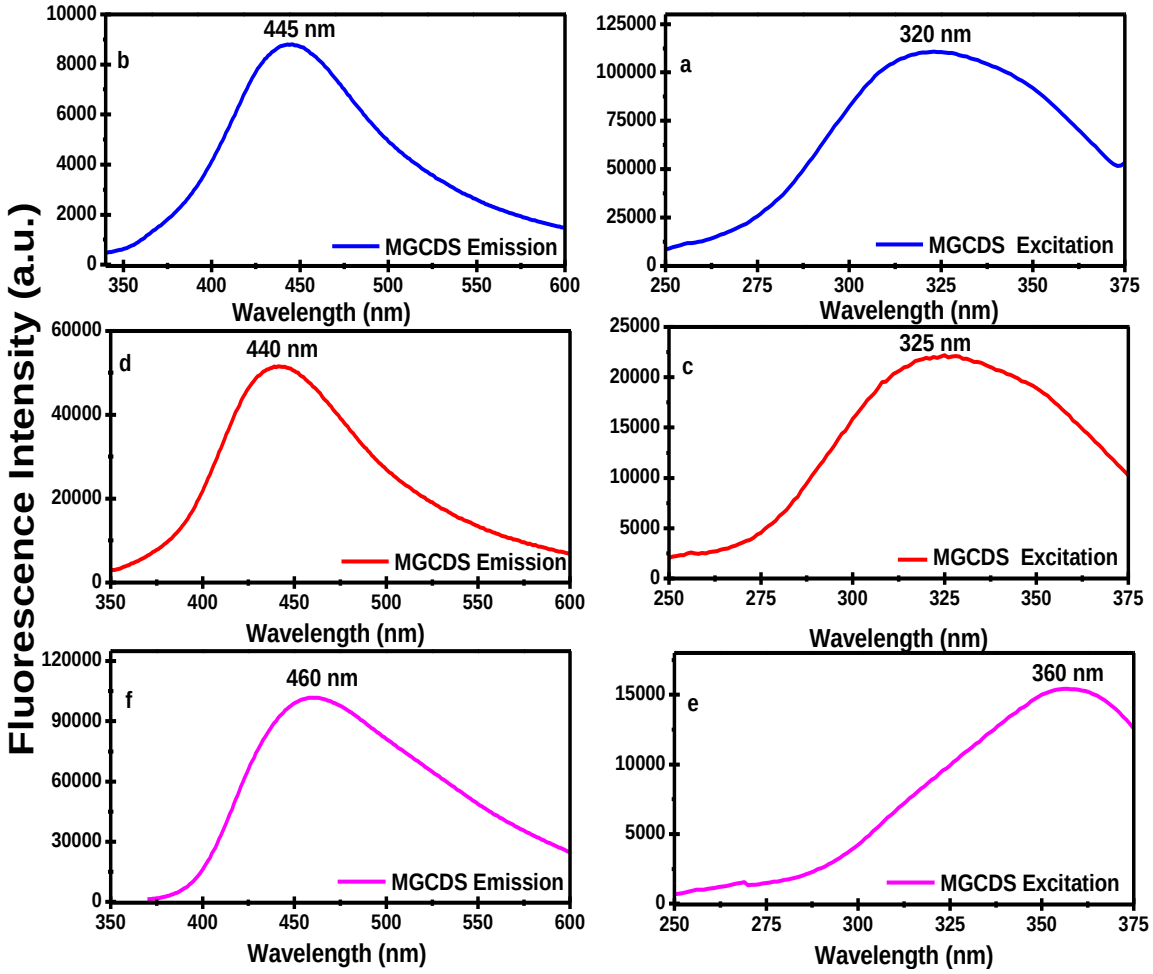

Fig. 4. Fluorescence spectra at different excitation it relative emission spectra of MGCDS

Thermogravimetric analysis

The thermal stability of the prepared MGCDs was examined using TGA. At temperatures reaching 150 °C, the MGCDs exhibited an initial weight reduction of 17%, attributed to the loss of moisture and water molecules from the sample. Subsequently, as the temperature increased to 200 °C, the MGCDs exhibited stable behaviour accompanied by a minor reduction in weight. The most significant weight loss of 49% occurred between 200 and 400 °C, which may be attributed to the degradation of surface functional groups such as carboxyl (–COOH) and carbonyl (C=O), as previously reported in similar carbon-based materials (Mintz *et al.* 2021). Upon increasing the temperature from 400 to 600 °C, further degradation occurred, resulting in an additional 16% weight loss.

In comparison, pure Moringa Gum (MG) showed an initial weight loss of 17% up to 150 °C, which can be attributed to the presence of moisture and hydroxyl (–OH) groups in the polymeric chain. The second major weight reduction occurred between 150 and 400 °C, where MG lost 49% of its mass due to thermal decomposition of biopolymer (Lofty *et al.* 2020). In the final stage, between 400°C and 600°C, MG exhibited an extensive weight loss of 14%, leading to a total decomposition of 80%, leaving only 20% residual mass. In contrast, MGCDs retained 35% of their mass at 600°C, suggesting improved thermal stability due to the formation of a more resilient carbonaceous structure.

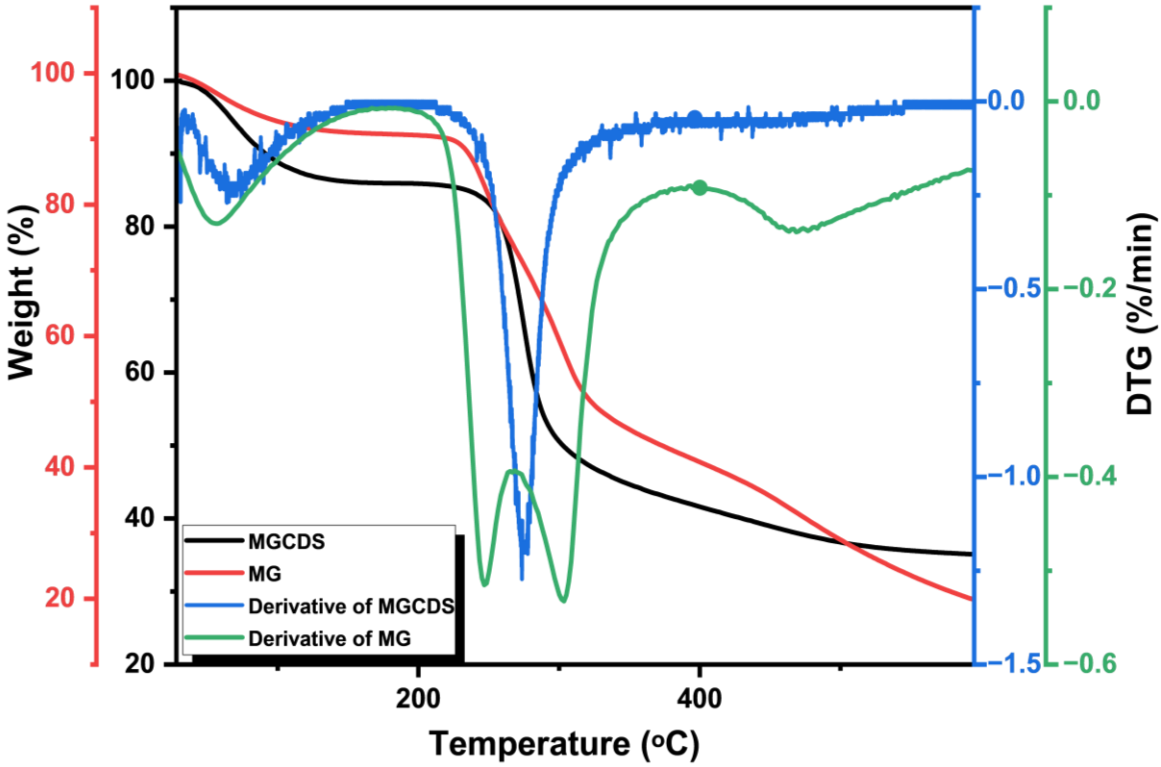

Fig. 5. TGA curves of Moringa Gum (MG) and MG-derived Carbon Dots (MGCDs). MG shows 80% total weight loss, while MGCDs exhibit improved thermal stability with 65% loss.

Zeta potential and hydrodynamic particle size

The stability and surface charge of Moringa gum-derived polymeric carbon dots (MGCDs) were evaluated through zeta potential measurements in different suspension media, including deionized (DI) water, Simulated Body Buffer (SBB), Phosphate Buffer Saline (PBS), and Dulbecco's Modified Eagle Medium (DMEM). The zeta potential values ranged from 23 ± 0.8 mV (DMEM) to 30 ± 0.8 mV (SBB), indicating a predominantly positive surface charge across all conditions. The relatively high zeta potential values (> ±25 mV) suggest that MGCDs exhibit good colloidal stability in these media due to sufficient electrostatic repulsion, minimizing aggregation. However, a slight decrease in zeta potential in DMEM (23 ± 0.8 mV) suggests that ionic interactions with the culture medium components might lead to minor charge screening effects.

The hydrodynamic size of MGCDs was assessed using dynamic light scattering (DLS), showing sizes ranging from 86 ± 3 nm (SBB) to 135 ± 4 nm (DMEM). The increase in hydrodynamic size in DMEM (135 ± 4 nm) suggests potential protein adsorption or

slight aggregation due to the complex ionic environment of the medium. In contrast, the relatively stable sizes in DI water (90 ± 2 nm) and PBS (89 ± 3 nm) indicate that the MGCDs maintain their dispersion properties effectively.

Table 1. Zeta Potential and Hydrodynamic Sizes of Moringa Gum-derived Polymeric Carbon Dots (MGCDs) Samples in Different Suspension Solutions

Sample	Zeta potential (mV) ± SD				Hydrodynamic size (nm) ± SD (nm)			
	DI water	SBB	PBS	DMEM	DI water	SBB	PBS	DMEM
(MGCDs)	29 ± 0.9	30 ± 0.8	28 ± 9	23 ± 0.8	90 ± 2	86 ± 3	89 ± 3	135 ± 4

DPPH radical activity

The DPPH scavenging capability of MGCDS was measured along with ascorbic acid (Ac) control. It seems that the DPPH scavenging capability of MGCDS was dosage dependent, with the highest inhibition occurring 85.03 ± 0.58 % at 0.9 mg/mL concentration. From the results in Fig. 6, it could be inferred that MGCDS show good scavenging potential, and they could possibly be used as radical inhibitors. Previously reports have shown the different inhibition patterns for carbon dots as they may differ in composition, luminescent properties and size.

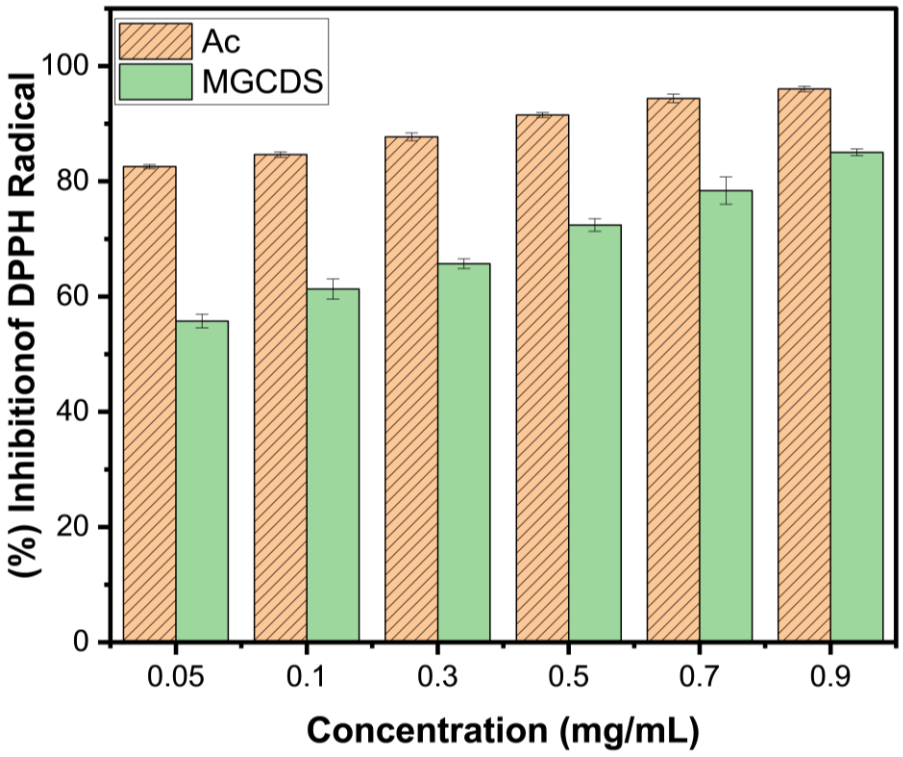

Fig. 6. DPPH radical scavenging activity of MGCDS and ascorbic acid

The DPPH scavenging ability of dots CDP prepared from curcumin showed a scavenging ability of 56% at 50 µg/mL concentrations (Pal *et al.* 2018). Another report highlights the preparation of carbon dots CQDs from bio-waste peels which showed the

scavenging potential of 23.3% at 5 mg/mL concentration (Rajamanikandan *et al.* 2022). Further, in the literature, ascorbic acid often exhibits higher DPPH radical scavenging activity than carbon dots (CDs) due to its direct electron donation mechanism, whereas CDs rely on surface functional groups for indirect radical neutralization. Ascorbic acid has a well-defined redox potential, enabling rapid radical quenching, while CDs exhibit slower electron transfer due to their size, surface charge, and functional group interactions . However, CDs offer long-term antioxidant stability and can be enhanced through surface modifications. This trend is consistent with previous studies, supporting the observed behavior in our results.

Antimicrobial activity

The antibacterial activity of prepared moringa gum carbon dots (MGCDS) was tested against the two bacterial strains at (20 mg/mL); 100 µL of the solution was loaded in the well against each strain to test the antibacterial potential of the luminescent carbon dots (Fig. 7). The ciprofloxacin disks 5µg (CT052B) from ThermoFisher were used as positive control. The MGCDS show good antibacterial activities against the tested strains (Table 1). The moringa based carbon dots showed more activity against *B. subtilis* with zone of inhibition 17.66 ± 0.57 mm as compared to *S. aureus* with a zone of inhibition 15.5 ± 0.5. In comparison the (ZOI) of pure moringa gum against the S. aureus was 13 mm at 40 mg/mL, with details listed in Table.2.

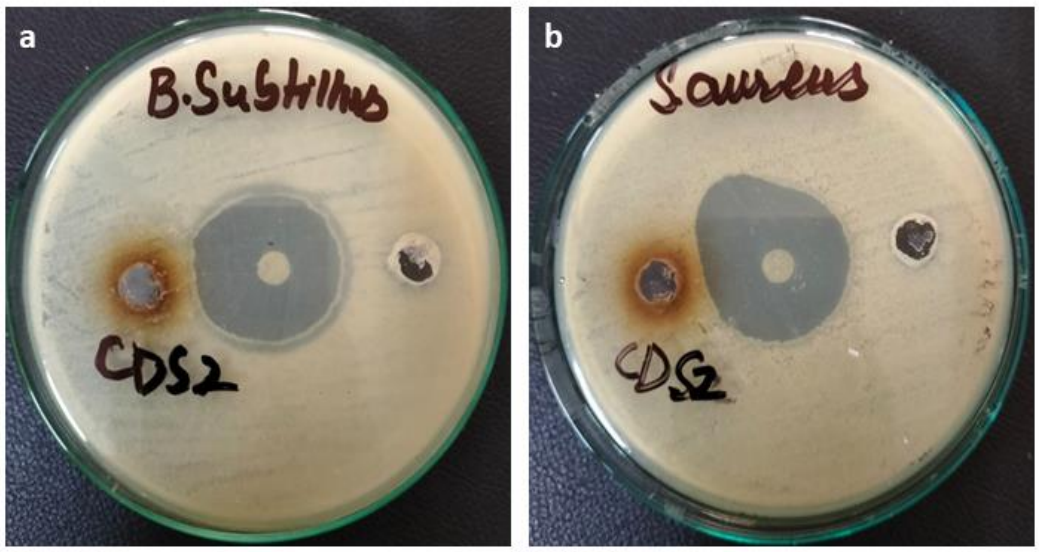

Fig. 7. (a) Antibacterial activity of MGCDS and ciprofloxacin as control against *B. subtilis* (b) Antibacterial activity of MGCDS and ciprofloxacin against *S. aureus*

Table 2. Inhibition Zones of MGCDS and Ciprofloxacin

Sample	Zone of Inhibition (mm ± SD)	
	B. subtilis	*S. aureus*
MGCDS (20 mg/mL)	17.66 ± 0.57	15.5 ± 0.5
Ciprofloxacin (10 µg/disk)	26.33 ± 0.57	26.83 ± 1.44

The novelty of this work is also defined from highlights of MGCDs synthesized *via* a microwave irradiation technique, as shown in Table 3, which is faster and more eco-

friendly than conventional hydrothermal and pyrolysis methods. Compared to bio-waste-derived carbon dots, MGCDs were found to exhibit high zeta potential, indicating better colloidal stability, and their bioactive nature makes them suitable for biomedical applications. Furthermore, while many bio-waste-derived CDs suffer from poor quantum yield and stability, MGCDs demonstrated superior performance in biocompatibility and surface charge, making them more promising for biological and environmental applications.

Table 3. Comparison of Moringa Gum-Derived Carbon Dots (MGCDs) with Bio-Waste-Based Nanomaterials

Precursor	Synthesis Method	Size (nm)	Zeta Potential (mV)	Fluorescence Quantum Yield (%)	Key Features	Reference
Moringa Gum	Microwave Irradiation (Rapid, Eco-Friendly)	90 ± 2	29 ± 0.9	20	Bioactive, High Stability, Biocompatible	Current Work
Orange Peels	Hydrothermal	5-10	-12	12	Low-cost, Non-toxic	(Prasannan and Imae 2013)
Banana Peels	Hydrothermal	3-8	-18	10	High Fluorescence, Poor Stability	(Atchudan *et al.* 2021)
Rice Husk	Pyrolysis	8-12	-25	15	Sustainable, Requires High Energy	(Ghosal *et al.* 2022)
Corn Starch	Microwave	7-11	20	25	Biodegradable, Moderate Stability	(Mary *et al.* 2022)

CONCLUSIONS

1. In this study, moringa gum-derived polymeric carbon dots (MGCDs) were successfully synthesized using a rapid, eco-friendly microwave irradiation technique. The MGCDs exhibited strong green fluorescence, excitation-dependent photoluminescence, and a UV-Vis absorption peak at ~290 nm, confirming their optical properties. The synthesized MGCDs demonstrated excellent antioxidant activity, achieving 87% DPPH scavenging efficiency at 0.9 mg/mL, comparable to ascorbic acid. Zeta potential analysis confirmed high colloidal stability, with values ranging from 23 ± 0.8 mV to 30 ± 0.8 mV, while hydrodynamic sizes varied between 86 ± 3 nm and 135 ± 4 nm depending on the suspension medium.
2. Structural characterization through X-ray diffraction (XRD) indicated an amorphous carbon nature, while thermogravimetric analysis (TGA) confirmed high thermal stability. The antibacterial activity of MGCDs was demonstrated against *Staphylococcus aureus* and *Bacillus subtilis*, with inhibition zones of 15.5 ± 0.5 mm and 17.66 ± 0.57 mm, respectively, at 40 mg/mL concentration. These results highlight the potential of MGCDs as cost-effective, multifunctional nanomaterials with applications in bioimaging, antimicrobial technologies, and fluorescent materials. The high stability, ease of synthesis, and strong bioactivity make MGCDs a promising

candidate for further biomedical and industrial applications.

ACKNOWLEDGMENTS

The authors acknowledge the services provided by the Central Hi-Tech Lab, Government College University Faisalabad, Pakistan for the instrumental analysis.

REFERENCES CITED

Ahmed, H. B., and Emam, H. E. (2020). "Environmentally exploitable biocide/fluorescent metal marker carbon quantum dots," *RSC Advances* 10(70), 42916-42929. DOI: 10.1039/D0RA06383E

Ahmed, H. B., El-Shahat, M., Allayeh, A. K., and Emam, H. E. (2023). "Maillard reaction for nucleation of polymer quantum dots from chitosan-glucose conjugate: Antagonistic for cancer and viral diseases," *International Journal of Biological Macromolecules*,224, 858-870. DOI: 10.1016/j.ijbiomac.2022.10.172

Ahmed, H. B., Emam, H. E., and Shaheen, T. I. (2024). "Fluorescent antimicrobial hydrogel based on fluorophore N-doped carbon dots originated from cellulose nanocrystals," *Scientific Reports* 14(1), article 29226.

Alabadi, A., Razzaque, S., Yang, Y., Chen, S., and Tan, B. (2015). "Highly porous activated carbon materials from carbonized biomass with high CO_2 capturing capacity," *Chemical Engineering Journal* 281, 606-612. DOI: 10.1016/j.cej.2015.06.032

Atchudan, R., Edison, T. N. J. I., Shanmugam, M., Perumal, S., Somanathan, T., and Lee, Y. R. (2021). "Sustainable synthesis of carbon quantum dots from banana peel waste using hydrothermal process for *in vivo* bioimaging," *Physica E: Low-Dimensional Systems and Nanostructures* 126, article 114417. DOI: 10.1016/j.physe.2020.114417

Basta, A. H., Lotfy, V. F., and Fathy, N. A. (2021). "Effective treatment for environmental enhancing the performance of undesirable agro-waste in production of carbon nanostructures as adsorbent," *Journal of Applied Polymer Science* 138(18), article 50350. DOI: 10.1002/app.50350

Bazazi, S., Hosseini, S. P., Hashemi, E., Rashidzadeh, B., Liu, Y., Saeb, M. R., Xiao, H., and Seidi, F. (2023). "Polysaccharide-based C-dots and polysaccharide/C-dot nanocomposites: Fabrication strategies and applications," *Nanoscale* 15(8), 3630-3650. DOI: 10.1039/D2NR07065K

Daoudi, W., Tiwari, A., Tyagi, M., Singh, P., Saxena, A., Verma, D. K., Dagdag, O., Sharma, H. K., Fuertes, P. O., and El Aatiaoui, A. (2024). "Carbon dots nanoparticles: A promising breakthrough in biosensing, catalysis, biomedical and authers applications," *Nano-Structures & Nano-Objects* 37, article 101074. DOI: 10.1016/j.nanoso.2023.101074

Demchenko, A. P. (2019). "Excitons in carbonic nanostructures," *Journal of Carbon Research* 5(4), article 71. DOI: 10.3390/c5040071

Ding, H., Wei, J.-S., Zhong, N., Gao, Q.-Y., and Xiong, H.-M. (2017). "Highly efficient red-emitting carbon dots with gram-scale yield for bioimaging," *Langmuir* 33(44),

12635-12642. DOI: 10.1021/acs.langmuir.7b02385

Emam, H. E., and Ahmed, H. B. 2021. "Antitumor/antiviral carbon quantum dots based on carrageenan and pullulan." *International Journal of Biological Macromolecules*, 170, 688-700. DOI: 10.1016/j.ijbiomac.2020.12.151

Emam, H. E., El-Shahat, M., Hasanin, M. S., and Ahmed, H. B. 2021. "Potential military cotton textiles composed of carbon quantum dots clustered from 4–(2,4–dichlorophenyl)–6–oxo–2–thioxohexahydropyrimidine–5–carbonitrile," *Cellulose* 28(15), 9991-10011. DOI: 10.1007/s10570-021-04147-4

Emam, H. E. (2022). "Clustering of photoluminescent carbon quantum dots using biopolymers for biomedical applications," *Biocatalysis and Agricultural Biotechnology* 42, article 102382. DOI: 10.1016/j.bcab.2022.102382

Emam, H. E., El-Shahat, M., Allayeh, A. K., and Ahmed, H. B. (2023). "Functionalized starch for formulation of graphitic carbon nanodots as viricidal/anticancer laborers," *Biocatalysis and Agricultural Biotechnology* 47, article 102577. DOI: 10.1016/j.bcab.2022.102577

Emam, H. E. (2024). "Carbon quantum dots derived from polysaccharides: Chemistry and potential applications," *Carbohydrate Polymers* 324, article 121503. DOI: 10.1016/j.carbpol.2023.121503

Feng, Z., Adolfsson, K. H., Xu, Y., Fang, H., Hakkarainen, M., and Wu, M. (2021). "Carbon dot/polymer nanocomposites: From green synthesis to energy, environmental and biomedical applications," *Sustainable Materials and Technologies* 29, article e00304. DOI: 10.1016/j.susmat.2021.e00304

Ghosal, S., Pani, P. K., Pattanaik, R. R., and Ghosal, M. K. (2022). "Mechanical characterization of concrete with rice husk-based biochar as sustainable cementitious admixture," in: *Recent Advances in Mechanical Engineering: Select Proceedings of ICRAMERD 2021*, 227-233. Springer Nature, Singapore.

Iqbal, Y., Chatha, S. A. S., Chauhdary, Z., Ijaz Hussain, A., and Khan, I. U. (2023). "Design and evaluation of moringa gum-based hydrogel dressings for cutaneous wound healing," *Journal of Bioactive and Compatible Polymers* 38(6), 417-436. DOI: 10.1177/08839115231199700

Jeong, M. J., Jin, S. W., Hwa, S. Y., Bang, H. O., Han, D. M., Jeon, J. Y., and Hwa, S. K. (2019). "Changes in the antioxidant potential of persimmon peel extracts prepared by different extraction methods," *Korean Journal of Medicinal Crop Science* 27(3), 186-193. DOI: 10.7783/KJMCS.2019.27.3.186

Ji, C., Zhou, Y., Leblanc, R. M., and Peng, Z. (2020). "Recent developments of carbon dots in biosensing: A review," *ACS Sensors* 5(9), 2724-2741. DOI: 10.1021/acssensors.0c01556

Kaczmarek, A., Hoffman, J., Morgiel, J., Mościcki, T., Stobiński, L., Szymański, Z., and Małolepszy, A. (2021). "Luminescent carbon dots synthesized by the laser ablation of graphite in polyethylenimine and ethylenediamine," *Materials* 14(4), article 729. DOI: 10.3390/ma14040729

Kolanowska, A., Dzido, G., Krzywiecki, M., Tomczyk, M. M., Łukowiec, D., Ruczka, S., and Boncel, S. (2022). "Carbon quantum dots from amino acids revisited: Survey of renewable precursors toward high quantum-yield blue and green fluorescence," *ACS Omega* 7(45), 41165-41176. DOI: 10.1021/acsomega.2c04751

Koutsogiannis, P., Thomou, E., Stamatis, H., Gournis, D., and Rudolf, P. (2020). "Advances in fluorescent carbon dots for biomedical applications," *Advances in Physics: X* 5(1), article 1758592. DOI: 10.1080/23746149.2020.1758592

Kumar, R., and Singh, B. (2024). "Functional network copolymeric hydrogels derived from moringa gum: Physiochemical, drug delivery and biomedical properties," *International Journal of Biological Macromolecules* 275, article 133352. DOI: 10.1016/j.ijbiomac.2024.133352

Mary, S. K., Koshy, R. R., Arunima, R., Thomas, S., and Pothen, L. A. (2022). "A review of recent advances in starch-based materials: Bionanocomposites, pH-sensitive films, aerogels, and carbon dots," *Carbohydrate Polymer Technologies and Applications* 3, article 100190. DOI: 10.1016/j.carpta.2022.100190

Mintz, K. J., Bartoli, M., Rovere, M., Zhou, Y., Hettiarachchi, S. D., Paudyal, S., Chen, J., Domena, J. B., Liyanage, P. Y., and Sampson, R. (2021). "A deep investigation into the structure of carbon dots," *Carbon* 173, 433-447. DOI: 10.1016/j.carbon.2020.11.017

Modi, P. D., Mehta, V. N., Prajapati, V. S., Patel, S., and Rohit, J. V. (2023). "Bottom-up approaches for the preparation of carbon dots," in: *Carbon Dots in Analytical Chemistry*, pp. 15-29, Elsevier, Amsterdam. DOI: 10.1016/B978-0-323-98350-1.00022-0

Mohanty, B., Verma, A. K., Claesson, P., and Bohidar, H. (2007). "Physical and anti-microbial characteristics of carbon nanoparticles prepared from lamp soot," *Nanotechnology* 18(44), article 445102. DOI: 10.1088/0957-4484/18/44/445102

Pal, T., Mohiyuddin, S., and Packirisamy, G. (2018). "Facile and green synthesis of multicolor fluorescence carbon dots from curcumin: *In vitro* and *in vivo* bioimaging and other applications," *ACS Omega* 3(1), 831-843. DOI: 10.1021/acsomega.7b01323

Prasannan, A., and Imae, T. (2013). "One-pot synthesis of fluorescent carbon dots from orange waste peels," *Industrial & Engineering Chemistry Research* 52(44), 15673-15678. DOI: 10.1021/ie402421s

Rajamanikandan, S., Biruntha, M., and Ramalingam, G. (2022). "Blue emissive carbon quantum dots (CQDs) from bio-waste peels and its antioxidant activity," *Journal of Cluster Science* 1-9. DOI: 10.1007/s10876-021-02029-0

Sailaja Prasannakumaran Nair, S., Kottam, N., and SG, P. K. (2020). "Green synthesized luminescent carbon nanodots for the sensing application of Fe^{3+} ions," *Journal of Fluorescence* 30(2), 357-363. DOI: 10.1007/s10895-020-02505-2

Sharma, A., Gadly, T., Neogy, S., Ghosh, S. K., and Kumbhakar, M. (2017). "Molecular origin and self-assembly of fluorescent carbon nanodots in polar solvents," *The Journal of Physical Chemistry Letters* 8(5), 1044-1052. DOI: 10.1021/acs.jpclett.7b00170

Sharma, N., Sharma, I., and Bera, M. K. (2022). "Microwave-assisted green synthesis of carbon quantum dots derived from *Calotropis gigantea* as a fluorescent probe for bioimaging," *Journal of Fluorescence* 32(3), 1039-1049. DOI: 10.1007/s10895-022-02923-4

Shibata, H., Abe, M., Sato, K., Uwai, K., Tokuraku, K., and Iimori, T. (2022). "Microwave-assisted synthesis and formation mechanism of fluorescent carbon dots from starch," *Carbohydrate Polymer Technologies and Applications* 3, article 100218. DOI: 10.1016/j.carpta.2022.100218

Wang, Q., Zhang, C., Shen, G., Liu, H., Fu, H., and Cui, D. (2014). "Fluorescent carbon dots as an efficient siRNA nanocarrier for its interference therapy in gastric cancer cells," *Journal of Nanobiotechnology* 12, 1-12. DOI: 10.1186/s12951-014-0058-0

Wang, Y., Guo, S., Sun, W., Tu, H., Tang, Y., Xu, Y., and Wu, J. (2024). "Synthesis of 4H-pyrazolo[3,4-d]pyrimidin-4-one hydrazine derivatives as a potential inhibitor for

the self-assembly of TMV particles," *Journal of Agricultural and Food Chemistry* 72(6), 2879-2887. DOI: 10.1021/acs.jafc.3c05334.

Yang, C., Xu, G., Hou, C., and Zhang, H. (2025). "Ratiometric fluorescence nanoprobe based on nitrogen-doped carbon dots for Cu^{2+} and Fe^{3+} detection," *Scientific Reports*, 15(1), article 6261. DOI: 10.1038/s41598-025-89327-z.

Zhang, H., Huang, H., Ming, H., Li, H., Zhang, L., Liu, Y., and Kang, Z. (2012). "Carbon quantum dots/Ag_3PO_4 complex photocatalysts with enhanced photocatalytic activity and stability under visible light," *Journal of Materials Chemistry* 22(21), 10501-10506. DOI: 10.1039/C2JM30703K

Zhou, J., Zhou, L., Chen, Z., Sun, J., Guo, X., Wang, H., and Zhang, X. (2025). "Remineralization and bacterial inhibition of early enamel caries surfaces by carboxymethyl chitosan lysozyme nanogels loaded with antibacterial drugs." *J. Dent.* 152, article 105489. DOI: 10.1016/j.jdent.2024.105489.

Zhu, S., Song, Y., Zhao, X., Shao, J., Zhang, J., and Yang, B. (2015). "The photoluminescence mechanism in carbon dots (graphene quantum dots, carbon nanodots, and polymer dots): Current state and future perspective," *Nano Research* 8, 355-381. DOI: 10.1007/s12274-014-0644-3

Article submitted: February 8, 2025; Peer review completed: March 15, 2025; Revised version received and accepted: March 25, 2025; Published: April 28, 2025.
DOI: 10.15376/biores.20.2.4479-4494